DMD Fast Forward. Published on February 21, 2013 as doi:10.1124/dmd.112.050120




## Title Page

# Elucidation of the Metabolic Pathways and the Resulting Multiple Metabolites of Almorexant, a Dual Orexin Receptor Antagonist, in Humans

Jasper Dingemanse, Petra Hoever, Matthias Hoch, Alexander Treiber, Winfried Wagner-Redeker, Tommaso Miraval, Gérard Hopfgartner, and Kasra Shakeri-Nejad

Departments of Clinical Pharmacology (JD, PH, MH, KS-N) and Preclinical Pharmacokinetics and Metabolism (AT), Actelion Pharmaceuticals Ltd, Allschwil, Switzerland and Swiss BioAnalytics AG (WW-R, TM, GH), Birsfelden, Switzerland

DMD Fast Forward. Published on February 21, 2013 as DOI: 10.1124/dmd.112.050120
This article has not been copyedited and formatted. The final version may differ from this version.



# Running Title Page

**Running title:** Metabolism and disposition of almorexant in humans

**Author for correspondence:** Dr. Jasper Dingemanse

Actelion Pharmaceuticals Ltd, Gewerbestrasse 16, 4123 Allschwil, Switzerland

Telephone: +41-61-565 6463

Fax: +41-61-565 6200

E-mail: jasper.dingemanse@actelion.com

Number of text pages: 24

Number of tables: 4

Number of figures: 7

Number of references: 20

Number of words in Abstract: 228

Number of words in Introduction: 482

Number of words in Discussion: 847

List of nonstandard abbreviations: $AUC_{0\text{-}inf}$, area under the plasma concentration-time curve from 0 to infinity; $AUC_{0\text{-}t}$, area under the plasma concentration-time curve from zero to time t of the last measured concentration above the limit of quantification; $C_{max}$, maximum plasma concentration; EDTA, ethylene diamine tetra-acetic acid; HPLC, high-performance liquid chromatography; LC-MS/MS, liquid chromatography/tandem mass spectrometry; $T_{max}$, time to maximum plasma concentration; $t_{1/2}$, terminal half-life.

## Abstract

Almorexant, a tetrahydroisoquinoline derivative, is a dual orexin receptor antagonist with sleep-promoting properties in both animals and humans. This study investigated the disposition, metabolism, and elimination of almorexant in humans. After oral administration of a 200-mg dose of $^{14}$C-almorexant, almorexant was rapidly absorbed ($T_{max}$ = 0.8 h) and the apparent terminal $t_{1/2}$ was 17.8 h. The radioactive dose was almost completely recovered with 78.0% of the administered radioactive dose found in feces and 13.5% in urine. Unchanged almorexant was not found in urine and represented 10% of the administered dose in feces. In total, 47 metabolites were identified of which 21 were shown to be present in plasma. There are 4 primary metabolites, the isomeric phenols M3 and M8, formed by demethylation, the aromatic isoquinolinium ion M5, formed by dehydrogenation, and M6, formed by oxidative dealkylation with loss of the phenylglycine moiety. Most of the subsequent products are formed by permutations of these primary metabolic reactions followed by conjugation of the intermediate phenols with glucuronic or sulfonic acid. The % of dose excreted in urine or feces for any of the metabolites did not exceed 10% of the administered radioactive dose nor did any of the metabolites represent more than 10% of total drug-related exposure. In conclusion, following rapid absorption, almorexant is extensively metabolized and excretion of metabolites in feces is the predominant route of elimination in humans.

DMD Fast Forward. Published on February 21, 2013 as DOI: 10.1124/dmd.112.050120
This article has not been copyedited and formatted. The final version may differ from this version.



## Introduction

Insomnia may be defined as the inability to sleep, in the absence of external impediments such as noise or bright light during the period when sleep should normally occur (PDR 1995). An estimated 10% of adults suffer from insomnia in the USA (NIH 2005) and most seek treatment. Current pharmacological treatments include barbiturates, benzodiazepine receptor agonists (benzodiazepines and non-benzodiazepines), and ramelteon, a melatonin receptor agonist (Zisapel 2012). Although the newer drugs such as non-benzodiazepines and ramelteon have an improved safety profile when compared to benzodiazepines and barbiturates (Zammit 2009), research is continuing to find new drugs with a new mechanism of action, a better tolerability, lower liability for abuse, without withdrawal effects, and improved sleep quality (Wafford and Ebert, 2008). Antagonism at orexin receptors is one of the new approaches pursued (Nishino 2007, Zisapel 2012).

The neuropeptides orexin-A and orexin-B were discovered in 1998 and are the endogenous ligands of two identified G-protein-coupled receptors, OX-1 and OX-2 (de Lecea et al, 1998; Sakurai et al, 1998). A number of experimental observations suggest that the orexin system plays an important role in the sleep-wake cycle and that antagonists of orexin receptors may enable sleep. These observations include the following: intracerebroventricular administration of orexin-A to rats enhanced arousal but decreased paradoxical sleep (Piper et al., 2000), cerebrospinal fluid levels of orexin-A are highest at the end of the wake period and lowest at the end of the sleep period (Kiyashchenko et al., 2002; Salomon et al., 2003), and deficits in normal orexinergic function play a major role in the pathogenesis of narcolepsy, a debilitating sleep disorder, in both animals and humans (Chemelli et al., 1999; Lin et al., 1999; Nishino et al., 2000).

Almorexant is a dual orexin receptor antagonist which has been shown to have promising sleep-promoting properties in animals, healthy subjects, and patients with

primary insomnia (Brisbare-Roch et al., 2007; Hoever et al., 2010, 2012b). The safety and pharmacokinetics of almorexant after single- and multiple-dose administration have been described previously (Hoch et al., 2012; Hoever et al., 2010; Hoever et al., 2012a). In brief, oral administration of almorexant was well tolerated with an adverse event profile consistent with that of a sleep-promoting drug (mainly somnolence and fatigue). The pharmacokinetics of almorexant are characterized by a clearance of 43 L/h, a large volume of distribution (683 L), a fast absorption ($T_{max}$ ~1 h), and a rapid disposition due to a pronounced distribution phase with concentrations decreasing to less than 20% of $C_{max}$ during the course of 8 hours. Despite a terminal $t_{1/2}$ of about 20 h, accumulation was minimal. Following evening administration, absorption was delayed ($T_{max}$ ~3 h) and $C_{max}$ decreased. The absolute bioavailability of almorexant is 11.4% which may indicate poor absorption and/or an extensive first-pass metabolism.

The purpose of the present study was to investigate the pharmacokinetics, routes of excretion, and metabolism of almorexant after oral administration to healthy male subjects.

DMD Fast Forward. Published on February 21, 2013 as DOI: 10.1124/dmd.112.050120
This article has not been copyedited and formatted. The final version may differ from this version.



## Materials and Methods

**Reference Compounds and Other Materials.** Almorexant ((2*R*)-2-{(1*S*)-6, 7-dimethoxy-1-[2-(4-trifluoromethyl-phenyl)-ethyl]-3,4-dihydro-1*H*-isoquinolin-2-yl}-*N*-methyl-2-phenyl-acetamide) was synthesized at Aptuit, Edinburgh, United Kingdom. The $^{14}$C-label of $^{14}$C-almorexant (ACT-078573E) was located at carbon 1 of the tetrahydroisoquinoline ring and the labeled compound was synthesized by Amersham Biosciences, Whitchurch, UK. For oral administration, almorexant was administered as a powder mix filled in hard gelatin capsules (content weight 450 mg). The capsules contained a mixture of non-radiolabeled and $^{14}$C-labeled almorexant that had been co-precipitated as powder to ensure homogeneous mixing and equivalent particle size.The specific radioactivity was 0.42 µCi/mg. A similar capsule formulation had also been used in several clinical trials (Hoever et al, 2010, 2012b). Nonlabeled almorexant, reference compounds ACT-078332 ((S)-6,7-dimethoxy-1-[2-(4-trifluoromethyl-phenyl)-ethyl]-1,2,3,4-tetra-hydroisoquinoline, M6), ACT-127979 ((R)-2-{(S)-7-hydroxy-6-methoxy-1-[2-(4-trifluoromethyl-phenyl)-ethyl]-3,4-dihydro-1*H*-isoquinolin-2-yl}-*N*-methyl-2-phenyl-acetamide, M8), ACT-127980 ((R)-2-{(S)-6-hydroxy-7-methoxy-1-[2-(4-trifluoromethyl-phenyl)-ethyl]-3,4-dihydro-1*H*-isoquinolin-2-yl}-*N*-methyl-2-phenyl-acetamide, M3), ACT-172515 (1-(6,7-dimethoxy-1-(4-(trifluoromethyl)phenethyl)isoquinolin-2-ium-2-yl)-2-(methylamino)-2-oxo-1-phenyl-ethan1-ide, M5), ACT-178291 (rac-7-methoxy-1-[2-(4-trifluoromethyl-phenyl)-ethyl]-1,2,3,4-tetrahydro-isoquinolin-6-ol, M7), ACT-208764 (2-(6,7-dimethoxy-1,2,3,4-tetrahydro-isoquinolin-1-yl)-1-(4-trifluoromethyl-phenyl)-ethanol, M31), ACT-208920 (6,7-dimethoxy-1-[2-(4-trifluoromethyl-phenyl)-ethyl]-isoquinoline, M27), ACT-242737 (2-[2-(6,7-Dimethoxy-1,2,3,4-tetrahydro-isoquinolin-1-yl)-ethyl]-5-trifluoromethyl-phenol, ACT-242987 (rac-5-[2-(6,7-Dimethoxy-1,2,3,4-tetrahydro-isoquinolin-1-yl)-

DMD Fast Forward. Published on February 21, 2013 as DOI: 10.1124/dmd.112.050120
This article has not been copyedited and formatted. The final version may differ from this version.



ethyl]-2-trifluoromethyl-phenol, ACT-244508 (1-((R)-6,7-dimethoxy-1,2,3,4-tetrahydro-isoquinolin-1-yl)-2-(4-trifluoromethyl-phenyl)-ethanol, ACT-254819 (rac-(1S*,4S*)-6,7-dimethoxy-1-[2-(4-trifluoromethyl-phenyl)-ethyl]-1,2,3,4-tetrahydro-isoquinolin-4-ol, M14b), ACT-285612 (rac-(1S*,4R*)-6,7--dimethoxy-1-[2-(4-trifluoromethyl-phenyl)-ethyl]-1,2,3,4-tetrahydro-isoquinolin-4-ol, M14a), and ACT-461759 ((S)-6-methoxy-1-[2-(4-trifluoromethyl-phenyl)-ethyl]-1,2,3,4-tetrahydro-isoquinolin-7-ol, M7 or isomer, and the internal standards d5-ACT-078573C, d5-ACT-127980A, d6-ACT-172515A, and d6-ACT-078332A, were synthesized at Actelion Pharmaceuticals Ltd (Allschwil, Switzerland). All the other chemicals and reagents used were obtained commercially.

**Subjects and Dosing.** The clinical part of this study was conducted at Covance (Allschwil, Switzerland), formerly called Swiss Pharma Contract, in full conformity with the principles of Good Clinical Practice and the Declaration of Helsinki and its amendments. Six male Caucasian subjects with a mean age of 50.7 years (range: 46 to 55 years) and a mean body mass index of 23.5 kg/m$^2$ (range: 20.2 to 27.3 kg/m$^2$) participated. After an overnight fast, all subjects received a single dose of 200 mg almorexant as a capsule containing 84 µCi of $^{14}$C-radioactivity and remained fasted for an additional 4 hours. To estimate the safe radioactive dose of $^{14}$C-labeled ACT-078573E administered as a single oral dose in male subjects, the radiation burden was estimated based on data from a preclinical distribution study with $^{14}$C-ACT-078573E in albino and pigmented rats as well as results of an excretion study with $^{14}$C-ACT-078573E in rats (Actelion Pharmaceuticals Ltd, data on file) and human pharmacokinetic data (Hoever et al, 2010). The dosimetry calculations, using FDA-approved Olinda software, yielded a radiation burden of 32.1 µSv/MBq. To account for interspecies differences and possible interindividual differences in bioavailability, a 5-fold safety factor was implemented resulting in an effective dose of 0.161 mSv/MBq. In general it is recommended not to

exceed a total radiation burden of 0.5 mSv in a mass balance study in healthy male subjects. The average environmental background radiation exposure in Switzerland is approximately 2.0 mSv per year. Therefore, the maximum dose of $^{14}$C-ACT-078573E-radioactivity was 3.11 MBq (84 μCi). The total radioactivity of each capsule prepared was measured to determine the individual radioactive dose, which varied from 83.05 to 83.24 μCi.

**Safety and tolerability.** Vital signs, ECG, physical examination, monitoring of adverse events, and clinical laboratory tests were assessed throughout the study. The investigator rated the intensity (mild, moderate, or severe) of all adverse events and the possible relationship (yes or no) to almorexant.

**Sample Collections.** For determination of $^{14}$C-radioactivity in whole blood and plasma, for the determination of the plasma concentrations of almorexant and 4 metabolites, M3, M5, M6, and M8, and for metabolic profiling about 15 mL blood was collected in light-protected tubes containing EDTA by direct venipuncture or via an intravenous catheter at the following time points: pre-dose and 0.17, 0.33, 0.5, 0.75, 1, 1.5, 2, 3, 4, 6, 8, 10, 12, 16, 24, 48, 72, 96, 120, 144, 168, 192, 216, and 240 h post-dosing. Expired air sampling was performed at the same time points (except for the 0.33-, 0.75-, and 1-hour time points) by letting the subjects expire into 4 mL of a trapping solution consisting of a 1:1 mixture of 1N hyamine hydroxide and ethanol with thymolphthalein as pH indicator. The subject expired into the solution until it became colorless, which indicated the neutralization of hyamine hydroxide by an equimolar amount of $CO_2$. Subsequently the vials were stored at + 4 ºC pending analysis for total radioactivity. Urine samples were collected at 8-h intervals on day 1 post-dosing and then at 24-h intervals on days 2 to 10. A 10-mL aliquot was used for scintillation counting and 4 x 10 mL aliquots were stored at −70°C for metabolic profiling. All feces was collected quantitatively for a

period of 10 days post-dosing and stored at −70°C as soon as possible. In the analyzing laboratory, thawed feces was homogenized in water and a sample corresponding to 300 mg was combusted prior to scintillation counting. The remainder was used for metabolic profiling. If on day 10 of the study, the recovery of total radioactivity was < 90% of the administered dose, sample collection had to continue until the set threshold of at least 90% was reached, or until no significant excretion could be detected, or the maximum number of 21 in-house days was reached.

**Measurement of Total Radioactivity.** Radioactivity in samples of whole blood, plasma, urine, feces, and expired air was determined in triplicate using a TRI-CARB 2800TR liquid scintillation counter (Perkin Elmer Life and Analytical Sciences, Waltham, MA). Whole blood samples were prepared by incubation for 2 h at 60°C with an ethanol/tissue solubilizer mixture (1:1) and then incubation for 30 min at room temperature after addition of hydrogen peroxide. Liquid scintillation fluid (Ultima Gold, Perkin Elmer Life and Analytical Sciences) was added and vials counted after having been allowed to stand in the dark at room temperature for at least 12 h. Plasma samples were first mixed with a small volume of water before scintillation fluid (Ultima Gold®) was added and radioactivity counted. Liquid scintillation fluid was added to urine (Ultima Gold®) and expired air (Aerosol-2, Perkin Elmer Life and Analytical Sciences, Downers Grove, IL) samples and radioactivity counted. Fecal extracts were homogenized in 2 equivalents of water (w/w) and 4 aliquots of approximately 300 mg were transferred to a porcelain cup and combusted using an OX-700 oxidizer (Zinsser Analytic GmbH, Frankfurt, Germany). The combusted material was taken up in scintillation fluid (Oxysolve-C-400, Zinsser Analytic, Berkshire, UK) and radioactivity determined. The performance of the radioactivity counting was monitored by running alongside quality control samples containing known activities of $^{14}$C-stearic acid (ARC-Inc., St. Louis, MO).

DMD Fast Forward. Published on February 21, 2013 as DOI: 10.1124/dmd.112.050120
This article has not been copyedited and formatted. The final version may differ from this version.



**Quantitative LC-MS/MS analysis.** Plasma concentrations of almorexant and its metabolites, M3, M5, M6, and M8, were determined using validated LC-MS/MS methods at Swiss BioAnalytics AG (Birsfelden, Switzerland). Two methods were developed to measure simultaneously all 5 analytes, one method using protein precipitation and one method using supported liquid extraction (SLE) for sample processing. The protein precipitation method had a calibration range from 0.4 to 100 ng/mL for almorexant, M5, and M6 and from 1.0 to 100 ng/mL for M3 and M8 (low calibration range). The SLE method had a range of 50.0 to 1000 ng/mL for all analytes (high calibration range).

For the high calibration range method, 300 µL of acetonitrile containing all 4 internal standards, i.e., penta-deuterated analogs of almorexant, M3, M5, and M6, were added to 100 µL plasma. The isomeric metabolites M3 and M8 were quantified using the same deuterated internal standard, i.e., ACT-127980A. Following protein precipitation and centrifugation, an equivalent volume of acetonitrile/methanol/water (5:5:90 v/v/v) was added and 10 µL of the diluted sample were injected onto the trapping column. The chromatographic system consisted of 2 pumps (Rheos 2000 and 2200, Thermo Fisher Scientific, Waltham, MA), a trapping column (Eclipse XDB-C18, 150 x 2.1 mm, 3.5 µm; Agilent, Palo Alto, CA), an analytical column (Eclipse XDB-C18, 30 x 4.6 mm, 3.5 µm; Agilent, Palo Alto, CA), and an autosampler (PAL; CTC Analytics, Zwingen, Switzerland). The solvent system for the trapping column consisted of solvent A, acetonitrile/water containing 1% formic acid, and solvent B, methanol. The column was eluted for 3 min with solvent A, then for 5 minutes with solvent B, and next for 5 min with solvent A. The solvent system for the analytical column consisted of solvent A, acetonitrile/methanol/water (5:5:90 v/v/v) containing 1% formic acid, and solvent B, acetonitrile/methanol/water (45:45:10 v/v/v) containing 1% formic acid. The column was

DMD Fast Forward. Published on February 21, 2013 as DOI: 10.1124/dmd.112.050120
This article has not been copyedited and formatted. The final version may differ from this version.



eluted for 7 min with a 70/30 mixture of solvents A and B, then for 4 min with solvent B, and next for 2 min with a 70/30 mixture of solvents A and B.

For the low calibration range method, 25 µL acetonitrile/water (20:80 v/v)/1% formic acid containing all 4 internal standards and 225 µL water + 2% formic acid were added to an aliquot of 250 µL plasma. After mixing, 300 µL of the diluted sample were applied to a 96-well Isolute SLE+ plate (Biotage Sweden AB, Uppsala, Sweden). After 10 min, low vacuum was applied to complete adsorption. Sample desorption was attained by applying 2 x 900 µL ethyl acetate. The final extract was evaporated to dryness and reconstituted in 100 µL acetonitrile/water (50:50 v/v) containing 1% formic acid and an aliquot of 20 µL was injected onto the HPLC column. The chromatographic system consisted of 2 pumps (Rheos 2000 and 2200, Thermo Fisher Scientific, Waltham, MA), an analytical column (XBridge C18, 50 x 2.1 mm, 3.5 µm; Waters, Milford, MA), and an autosampler (PAL; CTC Analytics, Zwingen, Switzerland). The solvent system for the analytical column consisted of solvent A, acetonitrile/methanol/water (5:5:90 v/v/v) containing 1% formic acid, and solvent B, acetonitrile/methanol/water (45:45:10 v/v/v) containing 1% formic acid. A gradient was used where solvent A was held at 80% for 0.5 min and then decreased to 0% in the next 4 min before re-equilibrium.

Mass spectrometric analysis was performed with a triple quadrupole mass spectrometer (TSQ Quantum; Thermo Fisher Scientific, Waltham, MA) operating in positive electrospray ionization mode with capillary temperature at 350°C and spray voltage at 4.0 kV. The performance of the methods was checked by the inclusion of quality control samples. Each analytical run was accepted when at least 2/3 of the quality control samples were within ± 15% of their nominal value and not more than 50% of the quality control samples at the same concentration were outside this limit.

DMD Fast Forward. Published on February 21, 2013 as DOI: 10.1124/dmd.112.050120
This article has not been copyedited and formatted. The final version may differ from this version.



**Pharmacokinetic analysis.** The pharmacokinetic evaluation for total radioactivity, almorexant and its 4 primary metabolites was performed with noncompartmental methods using WinNonlin version 5.2.1 (Pharsight, Mountain View, CA, USA). $C_{max}$ and $T_{max}$ were directly read from the plasma concentration-time profiles and the area under the concentration-time curve (AUC) was estimated using the linear trapezoidal rule and extrapolation to infinity with the help of the terminal elimination rate constant $\lambda_z$. The latter was determined by log-linear regression analysis of the terminal phase. The terminal half-life ($t_{½}$) was calculated by dividing ln2 by $\lambda_z$. Pharmacokinetic parameters were analyzed descriptively, calculating geometric means and 95% confidence limits or median and range for $T_{max}$.

**Sample Preparation for In Vivo Metabolic Profiling.** Due to the low radioactivity, plasma samples from all 6 subjects and of at least 2 time points were pooled. Similarly, urine samples were pooled but all time points were treated separately except for samples 0-16 h, 144-216 h, and 216-384 h which combined 2 or more time points. Pooled feces samples were prepared by combining a fixed percentage by weight from all 6 subjects using the following intervals; 0-48 h, 48-96 h, 96-144 h, 144-192 h, and 192-332 h.

To an aliquot of 2.5 mL plasma pool, 7.5 mL of acetonitrile were added. After protein precipitation at room temperature, plasma samples were centrifuged for 20 min at 4000 rpm and 8 °C and the supernatant collected. The protein pellet was resuspended with 7.5 mL of acetonitrile and the resulting suspension vortexed and centrifuged for 20 min at 4000 rpm and 8 °C. This procedure was repeated twice. The supernatants were combined and evaporated to dryness and reconstituted with 250 µL of water/methanol (50:50, v/v). An aliquot of 100 µL was injected onto the HPLC system. Two aliquots of 25 µL were taken for liquid scintillation counting to determine the procedural recovery which was

DMD Fast Forward. Published on February 21, 2013 as DOI: 10.1124/dmd.112.050120
This article has not been copyedited and formatted. The final version may differ from this version.



78.2%. The urine pools were analyzed without additional sample preparation. A 500-μL aliquot of each pool was injected onto the HPLC system while procedural recovery was 95.3%. Pooled feces were extracted by addition of three equivalents (w/v) of acetonitrile and vortex-mixing for approximately 30 min. Samples were then centrifuged for 20 min at 4000 rpm and 8°C. After centrifugation, the supernatant was decanted off. The pellet was extracted two more times as described above. Supernatants were combined and evaporated to dryness and reconstituted in 0.5 mL of water/methanol (50:50, v/v). A 100-μL aliquot was injected onto the HPLC system. Duplicate aliquots of 50 μL were used for liquid scintillation counting to determine procedural recovery which was 73.0%.

**Metabolite Profiling Analysis.** The metabolite profile of sample extracts was analyzed by LC-MS/MS combined with offline radioactivity detection after fraction collection. The LC-MS/MS/radioactivity detection system consisted of a PAL (CTC Analytics AG, Zwingen, Switzerland) autosampler, a Rheos 2200 (Thermo Fisher Scientific, Waltham, MA) pump, a Gecko-2000 (Cluzeau Info Lab, Courbevoie, France) column oven, a Luna C18 (4.6 x 250 mm, 5 μm; Phenomenex, Aschaffenburg, Germany) column, a LTQ linear ion trap (Thermo Fisher Scientific, Waltham, MA) mass spectrometer, and a FC204 (Gilson Inc., Middleton, WI) fraction collector. The system was operated by Xcalibur 2.0 software (Thermo Fisher Scientific, Waltham, MA). The postcolumn flow was split at a ratio of 1:5 between the mass spectrometer and the fraction collector. Fractions were sampled into 96-well plates, which were preconditioned with solid phase scintillation material (Deepwell Luma Plates; PerkinElmer Life and Analytical Sciences, Shelton, CT). The fraction collection interval was 0.15 min. After evaporation to dryness, the plates were analyzed by scintillation counting using a microplate counter (TopCount NXT; PerkinElmer Life and Analytical Sciences, Waltham, MA). Radiochromatograms were reconstructed by conversion of raw data (counts per fraction

versus fraction number) into chromatographic data (counts per fraction versus retention time) and processed by the Laura 4.0.3 (LabLogic Systems Limited, Sheffield, South Yorkshire, UK) software. Chromatographic peaks in the reconstructed radiochromatograms were manually integrated. Metabolites were quantified by calculating the percentage of each integrated radiopeak relative to the sum of all peaks in the radiochromatogram. Several metabolites co-eluted and were consequently quantified together. The LTQ mass spectrometer was operated in data-dependent mode. In this mode, the instrument was able to collect full scan and $MS^n$ data simultaneously, if an ion exceeded a predefined threshold.

Similar chromatography was used for urine and plasma samples. Metabolites were separated by a gradient of aqueous ammonium formate (50 mM pH 4.0, solvent A) versus acetonitrile (solvent B) at a flow rate of 1.0 mL/min. The gradient for plasma was 75% A at 0 min, 27% A at 45 min, 5% A at 45.5 and 50 min, and 75% A at 50.1 and 57 min. For urine the gradient was 90% A at 0 and 2 min, 30% A at 50 min, 5% A at 50.1 and 55 min, and 90% A at 55.1 and 60 min. For feces samples, solvent A was the same but solvent B consisted of methanol/acetonitrile (50:50 v/v). The gradient was 70% A at 0 min, 15% A at 50 min, 5% A at 50.1 and 55 min, and 70% A at 55.1 and 60 min at a flow rate of 1.0 mL/min. The mass spectrometer was operated in positive and negative electrospray ionization modes with capillary temperature at 275°C and spray voltage at 3.0 kV (positive mode) or 2.5 kV (negative mode).

**Structure Elucidation of Metabolites.** Structure elucidation of metabolites was done in several ways. In total 14 synthetic references were available for investigation of chromatographic retention times and MS and $MS^n$ spectra. Some metabolites were identified by comparing the data of these reference compounds with the corresponding data of compounds detected in the study samples. As the structure of the synthetic

DMD Fast Forward. Published on February 21, 2013 as DOI: 10.1124/dmd.112.050120
This article has not been copyedited and formatted. The final version may differ from this version.



reference compounds was known, their $MS^n$ spectra were used to investigate the fragmentation pathways and to assign structures to the various product ions. The $MS^n$ spectra of the synthesized reference compounds ACT-078573, ACT-127980 (M3), ACT-127979 (M8), ACT-172515 (M5), ACT-078332 (M6), ACT-285612 (M14a), ACT-254819 (M14b), ACT-208764 (M31), ACT-208920 (M27), ACT-178291 (M7 rac), and ACT-461759 (M7) are given in the supplement (Supplementary Figures 1-10) as well as the structure of the key fragments of ACT-078573 and its metabolites (Supplementary Table 1) suggested by Mass Frontier 6.0 (Thermo Fisher Scientific, Waltham, MA). This correlation between fragment masses and fragment structures facilitated the interpretation of $MS^n$ spectra of unknowns. In several instances the proposed structures and fragmentation pathways were further confirmed by accurate mass MS and $MS^n$ experiments with a LTQ Orbitrap (Thermo Fisher Scientific, Waltham, MA) mass spectrometer. Fractions that contained the metabolite of interest were pooled, evaporated to dryness under a steam of nitrogen, reconstituted in water/MeOH (50:50, v/v), and analyzed with an Orbitrap-LC/MS/MS. The resolving power was 100'000 and the mass accuracy in these experiments was usually better than 3 ppm.

In order to differentiate between hydroxy- and N-oxide metabolites, the respective metabolites were isolated by fractionation and subjected to H/D exchange. In the presence of excess of deuterium, OH-groups will undergo H/D exchange, while N-oxides will not.

Almorexant itself as well as selected metabolites may undergo further biotransformation by addition of glutathione. The formation of these metabolites as well as their downstream glycyl cysteine, N-acetylcysteine, and cysteine products was investigated by searching for the corresponding mass traces in the chromatograms of the study samples and comparing them to the respective mass traces in blank matrix chromatograms.

DMD Fast Forward. Published on February 21, 2013 as DOI: 10.1124/dmd.112.050120
This article has not been copyedited and formatted. The final version may differ from this version.



## Results

**Safety and Tolerability of Almorexant.** All 6 subjects completed the study and single-dose treatment with 200 mg $^{14}$C-almorexant was well tolerated. Fourteen adverse events were reported of which fatigue (6/6 subjects) and headache (2/6 subjects) were the most frequent. There were no severe or serious adverse events reported in this study and all adverse events resolved without sequelae. No clinically significant abnormalities were observed in clinical laboratory, vital signs, or ECG variables.

**Pharmacokinetics and Disposition of Almorexant.** The concentration-time profiles of total radioactivity in plasma and whole blood were characterized by rapid absorption with maximum concentrations of total radioactivity attained after 1.0 h (Figure 1a, Table 1). The mean terminal $t_{½}$ of total radioactivity in plasma was 78.0 h, which was longer than the $t_{½}$ of total radioactivity in whole blood (39.0 h). The exposure ratio based on $AUC_{0\text{-}inf}$ of total radioactivity in whole blood to plasma was 0.51 indicating that most of the radioactivity was associated to plasma.

Mean plasma concentration-time profiles of almorexant and its primary metabolites M3, M5, M6, and M8 are depicted in Figure 1b. Following oral administration, almorexant was rapidly absorbed as shown by a median $T_{max}$ of 0.8 h. Following attainment of $C_{max}$, plasma concentrations of almorexant declined with a marked disposition phase followed by an elimination phase characterized by a $t_{½}$ of 17.8 h. The $C_{max}$ of almorexant (113 ng/mL) was markedly lower than that of total radioactivity in plasma (1060 ng-equivalents/mL) suggesting that almorexant is extensively metabolized. This notion is further supported by the longer $t_{½}$ of total radioactivity in plasma and whole blood when compared to that of almorexant (Table 1).

**Mass Balance and Excretion in Feces and Urine.** The cumulative excretion profile of radioactivity in urine and feces as well as the total excretion (feces and urine) is

DMD Fast Forward. Published on February 21, 2013 as DOI: 10.1124/dmd.112.050120
This article has not been copyedited and formatted. The final version may differ from this version.



shown in Figure 2. Excretion of $^{14}$C-labeled material was virtually complete within 5 days in 5 out of 6 subjects whereas in one subject fecal recovery was delayed by about 4 days. The mean (range) recovery of the administered dose was 91.5% (88.2 - 94.1%), with 13.5% (9.6 - 17.5%) excreted in urine and 78.0% (74.4 - 81.4%) excreted in feces. The radioactivity excreted in expired air was < 0.5% of the administered radioactive dose in all subjects and was not taken into account for the calculation of total recovery.

**Quantitative Profiles of $^{14}$C-almorexant and Metabolites in Plasma and Excreta.** Representative radiochromatograms in plasma, urine, and feces are shown in Figure 3. Characterization of the metabolites presented was based on both MS data and retention time. Plasma pharmacokinetic variables of almorexant and identified metabolites in plasma are shown in Table 2 and the percentages of dose excreted in urine and feces are displayed in Table 3. As chromatographic baseline separation could not be achieved for all metabolites in the pooled plasma, urine, and feces samples, metabolites with similar retention times were grouped for the data analysis. To calculate the relative exposure to each circulating metabolite or groups of co-eluting metabolites, measured radioactivity in each pooled plasma sample was converted into ng-equivalents/mL and used to calculate the AUC from 0 to the last time point with a measurable concentration *($AUC_{0-t}$)*. As a consequence of this approach, the results may differ from those obtained with LC-MS/MS used in the pharmacokinetic analysis. In plasma, the main circulating entity was the combination M11/M41 followed by the combination M7/M14a/M31/M32 and by M30 which represented 15.6%, 3.2%, and 1.4%, respectively, of total radioactivity in plasma. Parent and all other metabolites or combination of metabolites accounted for less than 1% of total radioactivity. Parent and less abundant metabolites could only be quantified up to 1.6-3.5 h after dosing whereas total radioactivity was measured up to 300 h after dosing. No parent compound was detected in urine. The combinations of metabolites

DMD Fast Forward. Published on February 21, 2013 as DOI: 10.1124/dmd.112.050120
This article has not been copyedited and formatted. The final version may differ from this version.



M11/M41/M58/M59 and M45/M46 accounted for more than 1% of the radioactive dose administered whereas all other metabolites or combinations of metabolites represented less than 1% of the dose. The most abundant compound in feces was parent which represented 10.0% of the radioactive dose administered. The combinations of metabolites M5/M35 and M66/M67 accounted for 8.6% and 9.1%, respectively, whereas all other metabolites or combinations of metabolites represented less than 5% of the administered radioactive dose.

Parent and its identified metabolites represented about 50% of the total administered radioactivity. Overall, 49.6%, 61.5%, and 21.6% of the radioactivity in feces, urine, and plasma, respectively, were identified, indicating the presence of as yet unidentified metabolites. This is caused by the large number of metabolic pathways of almorexant. Importantly, all metabolites >1% of the total radioactivity in plasma and urine and > 5% in feces were identified. Analytical recovery was between 73.0% and 95.3% for the three matrices, indicating that no major metabolites have been missed by losses during sample preparation and LC/MS analysis.

**Structure Elucidation of Metabolites.** M3, M5, M6, M7, M8, M14a, M14b, M27, and M31 were identified by comparing chromatographic retention times and $MS^n$ spectra of available reference compounds with the corresponding data of the study samples. The structure proposals for M10, M11, M12, M28/29, M30, M32, M34, M39, and M41 were derived from interpretation of the respective $MS^n$ data, as described in the corresponding Materials and Methods section. H/D exchange experiments were performed for M35 and M37, indicating that oxidation occurred at a carbon atom rather than by formation of N-oxides. The major fragmentation reactions of protonated almorexant, m/z 513, are shown in Figure 4. The reactions are dominated by direct cleavages whereas rearrangement

DMD Fast Forward. Published on February 21, 2013 as DOI: 10.1124/dmd.112.050120
This article has not been copyedited and formatted. The final version may differ from this version.



reactions are of minor importance. This simplified the interpretation of spectra of unknown metabolites.

The metabolic scheme of the formation of the primary almorexant metabolites is displayed in Figure 5. Figure 6 presents the proposed metabolic schemes of almorexant in human plasma, feces, and urine for a) the M3-pathway, b) the M8-pathway, and c) and d) the M5- and M6-pathways, respectively. As mass spectrometry is usually not able to differentiate between isomeric structures, the site of a biotransformation reaction is not specified in this scheme if several possibilities existed and no reference compounds were available for comparison.

The metabolic scheme in human plasma is depicted in Figure 7a. Twenty-one discrete metabolite structures are present in human plasma. Some metabolite structures appeared to be close to a 10% level relative to parent almorexant. Twelve of these 21 metabolites are products of phase I biotransformations, while nine metabolites are phase II conjugates with either glucuronic acid or sulfonic acid. Figure 7b depicts the metabolic scheme in human urine and feces.

DMD Fast Forward. Published on February 21, 2013 as DOI: 10.1124/dmd.112.050120
This article has not been copyedited and formatted. The final version may differ from this version.



## Discussion

The safety and pharmacokinetic profile of almorexant, a dual orexin receptor antagonist, and its sleep-promoting properties warranted further investigation of this compound (Brisbare-Roch et al., 2007; Hoever et al., 2012b). This study was conducted to characterize the disposition and metabolism of almorexant in vivo. In addition, results of several supporting *in vitro* experiments are reported.

After oral administration of $^{14}$C-almorexant, only 10% of the administered dose (200 mg, 84 µCi) was recovered in feces as unchanged almorexant. Based on the assumptions that this 10% represents unabsorbed material and that intestinal bacteria do not metabolize almorexant, and together with the finding that in urine no unchanged almorexant was found, this suggests that at least 90% of the administered dose was absorbed and subsequently excreted as metabolites. The measured absolute bioavailability of almorexant in humans is only 11.4% (Hoch et al., 2012) and this discrepancy is readily explained by extensive first-pass metabolism, in line with its clearance of 43 L/h. After quick oral absorption ($T_{max}$ of 0.8 h), systemic almorexant concentrations decreased rapidly whereas the terminal $t_{1/2}$ of 17.8 h only represented a small part of the *AUC*. However, the plasma $t_{1/2}$ of total radioactivity was 4.4 times longer suggesting the presence of metabolites with longer half-lives than parent. Three (M3, M5, and M8) of the 4 metabolites measured in plasma by LC-MS/MS showed a longer $t_{1/2}$ than almorexant. Because of the difference in quantification limit of the method used, total radioactivity in whole blood could only be quantified up to 96 h after dosing whereas in plasma this was up to 240 h. This may explain the observed difference in $t_{1/2}$ between both matrices (39.0 h versus 78.0 h). The exposure ratio based on $AUC_{0\text{-}inf}$ of total radioactivity in whole blood to plasma was 0.51 and in line with the results of *in vitro* blood-to-plasma partitioning experiments.

DMD Fast Forward. Published on February 21, 2013 as DOI: 10.1124/dmd.112.050120
This article has not been copyedited and formatted. The final version may differ from this version.



The primary metabolites of almorexant are the isomeric phenols M3 and M8, formed by oxidative demethylation, the aromatic isoquinolinium ion M5, formed by dehydrogenation, and M6, formed by oxidative dealkylation with loss of the phenylglycine moiety. From these primary metabolites all other metabolites are derived involving a number of phase II enzyme reactions such as glucuronidation and sulfation among other reactions. In total 47 metabolites were identified and of these, 22 were identified in plasma. Ten metabolites, including the primary metabolite M6, were found in plasma but not in the excreta, which is most likely due to their low abundance. Only the co-eluting pair M11/M41 was observed at a plasma exposure greater than 10% of total radioactivity exposure (Table 2) whereas the majority was below 1%. M11 is a glucuronide of M7 and M41 is a glucuronide of M42 and both were found in urine. Based on the current ICH guideline (2009), those metabolites which have a plasma exposure of at least 10% of drug-related material are to be toxicologically characterized, i.e., preferably covered by exposure in preclinical toxicology studies. In rat toxicology studies M11/M41, which are both N-dealkylated, O-demethylated, and O-glucuronidated metabolites, showed higher exposure levels than in this clinical study. Further, O-glucuronides generally do not raise toxicology/safety concerns. The earlier so-called MIST guidance (FDA 2008) specified the threshold as 10% of parent drug. Obviously, for a highly metabolized drug such as almorexant this makes a big difference and would lead to practical challenges when a spectrum of metabolites, which as such reach low concentrations but still higher than 10% of those of parent drug, would have to be characterized. Therefore, the current ICH guidance appears to be more realistic.

Metabolism and subsequent biliary excretion of metabolites was identified as the major route of elimination. In feces, 16 metabolites were identified among which M3, M5, and M8 were among the more abundant ones together with M35 and M66/M67. Urinary

excretion represented a minor excretion pathway with, on average, 13.5% of the radioactivity administered recovered in urine. Unchanged almorexant was not found in urine and none of the 16 and 21 identified metabolites in feces and urine, respectively, were major, i.e., none represented > 10% of the administered radioactive dose. Therefore, and although most radioactive material in feces and especially urine was not identified, no further attempts were undertaken to characterize this unidentified material. When comparing the metabolic profile of almorexant established in the present study to that obtained in animals, no unique human metabolites were identified [Actelion Pharmaceuticals Ltd, data on file].

The exposure to the primary metabolites M3, M5, and M8 was approximately similar to that to almorexant whereas that to M6 was considerably higher. *In vitro* binding experiments have shown that M5 and M6 have no affinity for orexin receptors and thus do not appear to contribute to the pharmacological actions of almorexant. In contrast and compared to almorexant, metabolites M3 and M8 have similar affinity to the $OX_2$ receptor but have a 9 to 34 times lower affinity to the $OX_1$ receptors. Both metabolites may contribute to the pharmacological actions of almorexant [Actelion Pharmaceuticals Ltd, data on file].

In conclusion, extensive metabolism and subsequent excretion of metabolites via the feces represents the major elimination pathway of almorexant.

## Acknowledgements

The authors thank Hamed Aissaoui and Ralf Koberstein (Actelion Pharmaceuticals Ltd, Allschwil, Switzerland) for the synthesis of reference compounds, Covance (Allschwil, Switzerland) with Michael Seiberling as principal investigator for the clinical conduct of the study, Elke Spieker, Sebastian Thomas, and Janine Wank (Swiss BioAnalytics, Allschwil, Switzerland) for the bioanalytical part and the total radioactivity measurements, and Paul van Giersbergen (Van Giersbergen Consulting, Wuenheim, France) for editorial assistance.

DMD Fast Forward. Published on February 21, 2013 as DOI: 10.1124/dmd.112.050120
This article has not been copyedited and formatted. The final version may differ from this version.



## Authorship Contributions

*Participated in research design:* Dingemanse, Hoever, Treiber, and Shakeri-Nejad

*Conducted experiments:* Hopfgartner, Redeker, Miraval

*Performed data analysis:* Shakeri-Nejad, Treiber, Hopfgartner, Redeker, Miraval

*Wrote or contributed to the writing of the manuscript:* Dingemanse, Hoever, Hoch, Treiber, Redeker, Hopfgartner, and Shakeri-Nejad

## References

Brisbare-Roch C, Dingemanse J, Koberstein R, Hoever P, Aissaoui H, Flores S, Mueller C, Nayler O, van Gerven J, de Haas SL, Hess P, Qiu C, Buchmann S, Scherz M, Weller T, Fischli W, Clozel M, Jenck F (2007) Promotion of sleep by targeting the orexin system in rats, dogs and humans. *Nat Med* **13**: 150-155.

Chemelli RM, Willie JT, Sinton CM, Elmquist JK, Scammell T, Lee C, Richardson JA, Williams SC, Xiong Y, Kisanuki Y, Fitch TE, Nakazato M, Hammer RE, Saper CB, Yanagisawa M (1999) Narcolepsy in orexin knockout mice: molecular genetics of sleep regulation. *Cell* **98:** 437-451.

de Lecea L, Kilduff TS, Peyron C, Gao X, Foye PE, Danielson PE, Fukuhara C, Battenberg EL, Gautvik VT, Bartlett FS 2nd, Frankel WN, van den Pol AN, Bloom FE, Gautvik KM, Sutcliffe JG (1998) The hypocretins: hypothalamus-specific peptides with neuroexcitatory activity. *Proc Natl Acad Sci USA* **95:** 322–327.

FDA guidance for industry. Safety testing of drug metabolites. US Department of Health and Human Services. February 2008.

Hoch M, Hoever P, Zisowsky J, Priestley A, Fleet D, Dingemanse J (2012) Absolute oral bioavailability of almorexant, a dual orexin receptor antagonist, in healthy human subjects. *Pharmacology* **89:** 53-57.

Hoever P, de Haas SL, Dorffner G, Chiossi E, van Gerven JM, Dingemanse J (2012a) Orexin receptor antagonism: an ascending multiple-dose study with almorexant. *J Psychopharmacol* **26:** 1071-1080.

Hoever P, de Haas S, Winkler J, Schoemaker RC, Chiossi E, van Gerven J, Dingemanse J (2010) Orexin receptor antagonism, a new sleep-promoting paradigm: an ascending single-dose study with almorexant. *Clin Pharmacol Ther* **87:** 593-600.

Hoever P, Dorffner G, Beneš H, Penzel T, Danker-Hopfe H, Barbanoj MJ, Pillar G, Saletu B, Polo O, Kunz D, Zeitlhofer J, Berg S, Partinen M, Bassetti CL, Högl B, Ebrahim IO, Holsboer-Trachsler E, Bengtsson H, Peker Y, Hemmeter UM, Chiossi E, Hajak G, Dingemanse J (2012b) Orexin receptor antagonism, a new sleep-enabling paradigm: A proof-of-concept clinical trial. *Clin Pharmacol Ther* doi: 10.1038/clpt.2011.370.

ICH Topic M3. Non-clinical safety studies for the conduct of human clinical trials and marketing authorization for pharmaceutical products. CPMP/ICH/286/95. June 2009.

Kiyashchenko LI, Mileykovskiy BY, Maidment N, Lam HA, Wu MF, John J, Peever J, Siegel JM (2002) Release of hypocretin (orexin) during waking and sleep states. *J Neurosci* **22:** 5282-5286.

Lin L, Faraco J, Li R, Kadotani H, Rogers W, Lin X, Qiu X, de Jong PJ, Nishino S, Mignot E (1999) The sleep disorder canine narcolepsy is caused by a mutation in the hypocretin (orexin) receptor 2 gene. *Cell* **98:** 365-376.

National Institutes of Health (2005) NIH State of the Science Conference statement on manifestations and management of chronic insomnia in adults. *Sleep* **28**: 1049–1057.

Nishino S (2007) The hypocretin/orexin receptor: therapeutic prospective in sleep disorders. *Expert Opin Investig Drugs* **16:** 1785–1797.

Nishino S, Ripley B, Overeem S, Lammers GJ, Mignot E (2000) Hypocretin (orexin) deficiency in human narcolepsy. *Lancet* **355:** 39-40.

Piper DC, Upton N, Smith MI, Hunter AJ (2000) The novel brain neuropeptide, orexin-A, modulates the sleep-wake cycle of rats. *Eur J Neurosci* 12:726-730.

Sakurai T, Amemiya A, Ishii M, Matsuzaki I, Chemelli RM, Tanaka H, Williams SC, Richardson JA, Kozlowski GP, Wilson S, Arch JR, Buckingham RE, Haynes AC, Carr SA, Annan RS, McNulty DE, Liu WS, Terrett JA, Elshourbagy NA, Bergsma

DJ, Yanagisawa M (1998) Orexins and orexin receptors: a family of hypothalamic neuropeptides and G protein-coupled receptors that regulate feeding behavior. *Cell* **92:** 573–585.

Salomon RM, Ripley B, Kennedy JS, Johnson B, Schmidt D, Zeitzer JM, Nishino S, Mignot E (2003) Diurnal variation of cerebrospinal fluid hypocretin-1 (Orexin-A) levels in control and depressed subjects. *Biol Psychiatry* **54:** 96-104.

Wafford KA, Ebert B (2008) Emerging anti-insomnia drugs: tackling sleeplessness and the quality of wake time. *Nat Rev Drug Discov* **7:** 530-540.

Zammit G (2009) Comparative tolerability of newer agents for insomnia. *Drug Saf* **32:** 735-748.

Zisapel N (2012) Drugs for insomnia. *Exp Opin Emerg Drugs* 17: 299-317.

## Footnotes

This work was funded by Actelion Pharmaceuticals Ltd, Allschwil, Switzerland.

DMD Fast Forward. Published on February 21, 2013 as DOI: 10.1124/dmd.112.050120
This article has not been copyedited and formatted. The final version may differ from this version.



## Figure Legends

**FIG. 1 a)** Mean (±SD) concentration-time profiles of total radioactivity in whole blood and plasma; **b)** Mean plasma concentration-time profiles of almorexant and its metabolites M3, M5, M6, and M8 after a single 200-mg oral administration of $^{14}$C-almorexant in healthy male human subjects (N=6). No SD is displayed.

**FIG. 2** Mean recovery (±SD) of almorexant-related material in the excreta after a single 200-mg oral administration of $^{14}$C-almorexant in healthy male human subjects (N=6).

**FIG. 3** a) Representative HPLC radiochromatograms of human plasma, Pool 2, 0.75-1 h (**I**), Pool 3, 1.5-2 h (**II**), and Pool 4 (3-4 h) (**III**); BLQ = 15 CPM (only quantifiable peaks are annotated), **b**) Representative HPLC radiochromatograms for feces, Pool 1, 0-48 h (**I**) and Pool 2, 48-96 h (**II**); BLQ = 25 CPM (only quantifiable peaks are annotated). and **c**) Representative HPLC radiochromatograms for urine, Pool 1, 0-48 h (**I**) and Pool 2, 48-96 h (**II**); BLQ = 25 CPM (only quantifiable peaks are annotated).
Characterization of the metabolites presented was based on both MS data and retention time.

**FIG. 4**

The MS/MS spectrum of almorexant and major fragmentation reactions of protonated almorexant, *m/z* 513.

**FIG. 5** Metabolism pathways of almorexant in humans after a single 200-mg oral administration of $^{14}$C-almorexant. Structures of metabolites were characterized by mass spectrometry. Four primary metabolites are the starting points for the entire metabolic

DMD Fast Forward. Published on February 21, 2013 as DOI: 10.1124/dmd.112.050120
This article has not been copyedited and formatted. The final version may differ from this version.



scheme, i.e., demethylation of either methoxy group in the 6- or 7-position of the tetrahydroisoquinoline ring to yield the isomeric phenols M3 and M8, dehydrogenation of the tetrahydroisoquinoline to the aromatic isoquinolinium ion M5, and oxidative dealkylation with loss of the phenylglycine moiety to yield M6.

**FIG. 6**

**a)** Proposed metabolic scheme of almorexant in human plasma, feces, and urine for the M3-pathway. The present organization of data is intended to visualize their interrelationship rather than claiming knowledge of the exact sequence of metabolic pathways. Comments on the potential existence of isomers are attached to those metabolites for which mass spectrometry is unable to identify the exact position of a structural modification or the presence of 1 or several isomers. P=plasma, U=urine, F=feces.

**b)** Proposed metabolic scheme of almorexant in human plasma, feces, and urine for the M8-pathway. The present organization of data is intended to visualize their interrelationship rather than claiming knowledge of the exact sequence of metabolic pathways. Comments on the potential existence of isomers are attached to those metabolites for which mass spectrometry is unable to identify the exact position of a structural modification or the presence of 1 or several isomers. P=plasma, U=urine, F=feces.

**c)** Proposed metabolic scheme of almorexant in human plasma, feces, and urine for the M5- and M6-pathway. The present organization of data is intended to visualize their interrelationship rather than claiming knowledge of the exact sequence of metabolic pathways. The structural information depicted in this scheme is based on the available

DMD Fast Forward. Published on February 21, 2013 as DOI: 10.1124/dmd.112.050120
This article has not been copyedited and formatted. The final version may differ from this version.



mass spectrometric raw data. Comments on the potential existence of isomers are attached to those metabolites for which mass spectrometry is unable to identify the exact position of a structural modification or the presence of 1 or several isomers. P=plasma, U=urine, F=feces.

**d)** Proposed metabolic scheme of almorexant in human plasma, feces, and urine for the M6-pathway. The present organization of data is intended to visualize their interrelationship rather than claiming knowledge of the exact sequence of metabolic pathways. The structural information depicted in this scheme is based on the available mass spectrometric raw data. Comments on the potential existence of isomers are attached to those metabolites for which mass spectrometry is unable to identify the exact position of a structural modification or the presence of 1 or several isomers. P=plasma, U=urine, F=feces.

**FIG. 7**

**a)** Phase I metabolites are labeled in light orange and phase II metabolites are labeled in dark orange. Due to their isomeric nature, the exact chemical structure of metabolites M10, M12, M32, and M35 could not be determined by mass spectrometry. To account for the existence of isomers, both possibilities (e.g., M12 and M12-i) have been included in Figure 5, yielding to symmetrical metabolic pathways for metabolites M3 and M8. [Mx] indicates intermediate metabolites that were not observed in humans.

**b)** Almorexant metabolites are organized by the number of metabolic steps required to yield their final chemical structure, i.e., each circle contains the metabolites requiring the same number of chemical modifications. Metabolites highlighted in yellow are those detected in urine (light yellow = phase I metabolites; dark yellow = phase II metabolites)

DMD Fast Forward. Published on February 21, 2013 as DOI: 10.1124/dmd.112.050120
This article has not been copyedited and formatted. The final version may differ from this version.



whereas those in brown were found in feces. [Mx] indicates intermediate metabolites that were not observed in humans. Most metabolites in this scheme are products of multi-step transformations. The present organization of data is intended to visualize their interrelationship rather than claiming knowledge of the exact sequence of metabolic pathways.

DMD Fast Forward. Published on February 21, 2013 as DOI: 10.1124/dmd.112.050120
This article has not been copyedited and formatted. The final version may differ from this version.



# Tables

**Table 1 Mean pharmacokinetic parameters of almorexant and its 4 primary metabolites in plasma and of total radioactivity in plasma and whole blood after a single 200-mg oral administration of $^{14}$C-almorexant in healthy male subjects.**

| | $C_{max}$ [ng/mL][a] | $T_{max}$ [h] | $t_{½}$ [h] | $AUC_{0\text{-}inf}$ [ng*h/mL][b] |
|---|---|---|---|---|
| **Almorexant** | 113 (74.8, 170) | 0.8 (0.5-1.0) | 17.8 (12.4, 25.7) | 262 (206, 333) |
| **ACT-078332 (M6)** | 99.4 (70.6, 140) | 1.5 (1.0-2.0) | 10.4 (9.04, 12.0) | 1039 (743, 1452) |
| **ACT-172515 (M5)** | 80.4 (59.1, 109) | 0.9 (0.8-1.5) | 26.3 (23.9, 28.9) | 282 (223, 356) |
| **ACT-127979 (M8)** | 61.4 (44.1, 85.4) | 1.0 (0.8-1.0) | 21.7 (14.2, 33.0) | 386 (283, 526) |
| **ACT-127980 (M3)*** | 25.7 (17.2, 38.4) | 0.8 (0.5-1.0) | 22.1 (11.1, 43.8) | 160 (102, 252) |
| **Radioactivity in whole blood** | 678 (561, 819) | 1.0 (1.0-2.0) | 39.0 (34.1, 44.5) | 26321 (22051, 31420) |
| **Radioactivity in plasma** | 1060 (871, 1291) | 1.0 (1.0-4.0) | 78.0 (66.2, 91.9) | 51547 (45940, 57839) |

Data are expressed as median (range) for $T_{max}$ and geometric mean (95% confidence interval) for $C_{max}$, $t_{½}$, and $AUC_{0\text{-}inf}$. N=6.

*For one subject $t_{1/2}$ could not be reliably estimated, N=5 for $t_{1/2}$ and $AUC_{0\text{-}inf}$.

a Unit for radioactivity in whole blood and plasma is ng-equivalents/mL.

b Unit for radioactivity in whole blood and plasma is ng-equivalents*h/mL.

DMD Fast Forward. Published on February 21, 2013 as DOI: 10.1124/dmd.112.050120
This article has not been copyedited and formatted. The final version may differ from this version.



**Table 2 Plasma pharmacokinetic variables of almorexant and metabolites after a single 200-mg oral administration of $^{14}$C-almorexant in healthy male subjects.**

| Compound | $T_{max}$ (h) | $C_{max}$ (ng.eq/mL) | $AUC_{0-t}$ (ng-eq*h/mL) | $t_{last}$ (h) | % of parent | % of total radioactivity |
|---|---|---|---|---|---|---|
| Almorexant | 0.9 | 66.6 | 61.2 | 1.6 | 100 | 0.11 |
| M3/M8 | 0.9 | 69.8 | 123 | 3.5 | 201 | 0.23 |
| M5/M27 | 0.9 | 44.1 | 44.8 | 1.6 | 73.2 | 0.08 |
| M6 | 1.6 | 49.0 | 331 | 11 | 541 | 0.61 |
| M7/M14A/M31/ M32 | 3.5 | 38.4 | 1720 | 60 | 2811 | 3.2 |
| M10/M12 | 0.9 | 65.0 | 62.8 | 1.6 | 103 | 0.12 |
| M11/M41 | 11 | 260 | 8460 | 60 | 13824 | 15.6 |
| M14b | 1.6 | 21.5 | 17.2 | 1.6 | 28.1 | 0.03 |
| M28/M29 | 0.9 | 42.5 | 18.6 | 0.9 | 30.4 | 0.03 |
| M30 | 3.5 | 45.0 | 731 | 20 | 1194 | 1.4 |
| M34/M35 | 1.6 | 55.0 | 61.0 | 1.6 | 100 | 0.11 |
| M37 | 1.6 | 21.5 | 17.2 | 1.6 | 28.1 | 0.03 |
| M39 | 1.6 | 26.0 | 20.8 | 1.6 | 34.0 | 0.04 |
| Total radioactivity | 1.6 | 1050 | 54100 | 300 | | |

A number of metabolites co-eluted in plasma as indicated.

DMD Fast Forward. Published on February 21, 2013 as DOI: 10.1124/dmd.112.050120
This article has not been copyedited and formatted. The final version may differ from this version.



**Table 3 Percentage of dose excreted in urine and feces of almorexant and its identified metabolites after a single 200-mg oral administration of $^{14}$C-almorexant in healthy male subjects.**

| Metabolite | Urine | Feces | Urine + feces |
|---|---|---|---|
| Parent | | 10.0 | 10.0 |
| M3/M8 | | 3.3 | 3.3 |
| M5/M35 | | 8.6 | 8.6 |
| M11/M41/M58/M59 | 3.82 | | 3.82 |
| M28/M29/M51 | 0.36 | | 0.36 |
| M30/M52/M63 | 0.34 | | 0.34 |
| M33/M34 | | 1.7 | 1.7 |
| M38/M68/M71 | | 1.9 | 1.9 |
| M39/M55 | 0.81 | | 0.81 |
| M42/M43 | | 0.9 | 0.9 |
| M44/M53 | 0.48 | | 0.48 |
| M45/M46 | 1.39 | | 1.39 |
| M48/M60/M61 | 0.33 | | 0.33 |
| M50 | 0.40 | | 0.40 |
| M57 | 0.41 | | 0.41 |
| M62 | | 0.8 | 0.8 |
| M65 | | 2.0 | 2.0 |
| M66/M67 | | 9.1 | 9.1 |
| M69 | | 0.4 | 0.4 |
| Total | 8.34 | 38.7 | 47.0 |

A number of metabolites co-eluted in feces or urine as indicated.

**Table 4 LC-MS/MS data of almorexant and metabolites detected in plasma, urine, and feces from healthy male subjects after a single 200-mg oral administration of $^{14}$C-almorexant.**

| Compound | $[M+H]^+$ formula | Metabolite identification | Characteristic Product Ions | Found in |
|---|---|---|---|---|
| Parent | 513, $C_{29}H_{32}F_3N_2O_3$ | | 482, 462, 454, 365, 349, 282, 192, 190 | P, F |
| M3 | 499, $C_{28}H_{29}F_3N_2O_3$ | O-demethylated | 468, 440, 351, 335 | P, F |
| M5 | 509, $C_{29}H_{28}F_3N_2O_3$ | didehydrogenated | 489, 450, 362, 342, 203 | P, F |
| M6 | 366, $C_{20}H_{23}F_3NO_2$ | N-dealkylated | 349, 190 | P |
| M7 | 352 | N-dealkylated, O-demethylated | 335, 315, 303, 176, 163, 137 | P |
| M8 | 499, $C_{28}H_{29}F_3N_2O_3$ | O-demethylated | 468, 440, 351, 335 | P, F |
| M10 | 675 | | 499, 468, 440, 351, 335 | P |
| M11 | 528, $C_{25}H_{29}F_3NO_8$ | N-dealkylated O-demethylated O-glucuronidated | 352, 335, 315, 303, 176, 163, 137 | P, U |
| M12 | 691 | | 673, 524, 515, 497, 348 | P |
| M14a/M14b | 382, $C_{20}H_{23}F_3NO_3$ | N-dealkylated, oxygenated, isomers | 364, 347, 192 | P |
| M27 | 362, $C_{20}H_{19}F_3NO_2$ | N-dealkylated, dehydrogenated | 347, 342, 203 | P |
| M28/M29 | 671 | isomers | 495, 475, 444, 348 | P, U |
| M30 | 432, $C_{19}H_{21}F_3NSO_5$ | N-dealkylated, O-demethylated, O-sulfated | 352, 315, 303, 176, 163, 137, 350, 335 | P, U |
| M31 | 382, $C_{20}H_{22}F_3NO_3$ | N-dealkylated, oxygenated | 364, 347, 208, 192, 165 | P |
| M32 | 675 | O-demethylated, glucuronidated | 499, 468, 440, 351, 335 | P |
| M33 | 495, $C_{28}H_{26}F_3N_2O_3$ | O-demethylated, didehydrogenated | 475, 444, 436, 348, 333, 328, 189 | F |
| M34 | 495, $C_{28}H_{26}F_3N_2O_3$ | N-demethylated, didehydrogenated | 475, 450, 362 | P, F |

| Compound | $[M+H]^+$ formula | Metabolite identification | Characteristic Product Ions | Found in |
|---|---|---|---|---|
| M35 | 531 | O-demethylated, oxygenated | 513, 501, 495, 475, 456, 353, 335, 323, 268 | P, F |
| M36 | 545 | | 527, 515, 509, 470, 367, 349, 282 | P |
| M37 | 515 | O-demethylated, oxygenated | 497, 341, 325, 324, 296, 207 | P |
| M38 | 515 | O-demethylated, oxygenated | 497, 348, 176 | F |
| M39 | 524, $C_{25}H_{25}F_3NO_8$ | N-dealkylated, didehydrogenated, O-demethylated, O-glucuronidated | 348, 328, 189 | P, U |
| M41 | 524, $C_{25}H_{25}F_3NO_8$ | N-dealkylated, didehydrogenated, O-demethylated, O-glucuronidated | 348, 328, 189 | P, U |
| M42/M43 | 348 | N-dealkylated, O-demethylated, didehydrogenated, isomers | 328, 189, 174, 160, 143 | F |
| M44 | 526, $C_{25}H_{27}F_3NO_8$ | dehydrogenated, glucuronidated | 350, 335, 191 | U |
| M45 | 526, $C_{25}H_{27}F_3NO_8$ | dehydrogenated, glucuronidated | 350, 335, 191, 190 | U |
| M46 | 528, $C_{25}H_{29}F_3NO_8$ | N-dealkylated, O-demethylated, glucuronidated | 352, 335, 315, 303, 176, 163, 137 | U |
| M47/M48 | 544 | N-dealkylated, oxygenated, glucuronidated, isomers | 368, 351, 331, 319, 192, 179, 153 | U |
| M49 | 546 | | 370, 353 | U |
| M50 | 657 | di-O-demethylated, didehydrogenated, glucuronidated | 481, 450, 348, 334 | U |
| M51/M52 | 657 | di-O-demethylated, didehydrogenated, | 481, 450, 334 | U |

| Compound | $[M+H]^+$ formula | Metabolite identification | Characteristic Product Ions | Found in |
|---|---|---|---|---|
| | | glucuronidated, isomers | | |
| M53 | 540 | N-dealkylated, didehydrogenated, oxygenated glucuronidated | 364, 346, 344, 205 | U |
| M55 | 540, $C_{25}H_{25}F_3NO_8$ | N-dealkylated, didehydrogenated, oxygenated glucuronidated | 364, 346 | U |
| M57 | 540 | N-dealkylated, didehydrogenated, oxygenated glucuronidated | 364, 349, 346 | U |
| M58 | 540, $C_{25}H_{25}F_3NO_9$ | N-dealkylated, didehydrogenated, O-demethylated, oxygenated, O-glucuronidated | 364, 349, 205 | U |
| M59 | 540, $C_{25}H_{25}F_3NO_9$ | N-dealkylated, didehydrogenated, O-demethylated, oxygenated, O-glucuronidated | 364, 344 | U |
| M60 | 538 | | 362, 347, 342, 203 | U |
| M61 | 558 | | 364, 347, 192 | U |
| M62 | 501 | di-O-demethylated, oxygenated | 483, 334, 424 | F |
| M63 | 350 | N-dealkylated, dehydrogenated | 335, 191 | U |
| M65 | 501 | di-O-demethylated, oxygenated | 483, 471, 426, 323, 303, 283 | F |
| M66 | 501 | di-O-demethylated, oxygenated | 483, 471, 426, 323, 303, 283 | F |
| M67 | 485, $C_{27}H_{28}F_3N_2O_3$ | di-O-demethylated | 454, 426, 386, 321, 254, 164 | F |
| M68 | 515 | O-demethylated, oxygenated | 484, 456, 351, 331, 319, 192, 179, 153 | F |
| M69 | 497, $C_{28}H_{28}F_3N_2O_3$ | O-demethylated, dehydrogenated | 348, 323 | F |

| Compound | $[M+H]^+$ formula | Metabolite identification | Characteristic Product Ions | Found in |
|---|---|---|---|---|
| M71 | 515, $C_{28}H_{30}F_3N_2O_4$ | O-demethylated, oxygenated | 497, 485, 440, 337 | F |

F = feces, P = plasma, U = urine

Figure 1

A

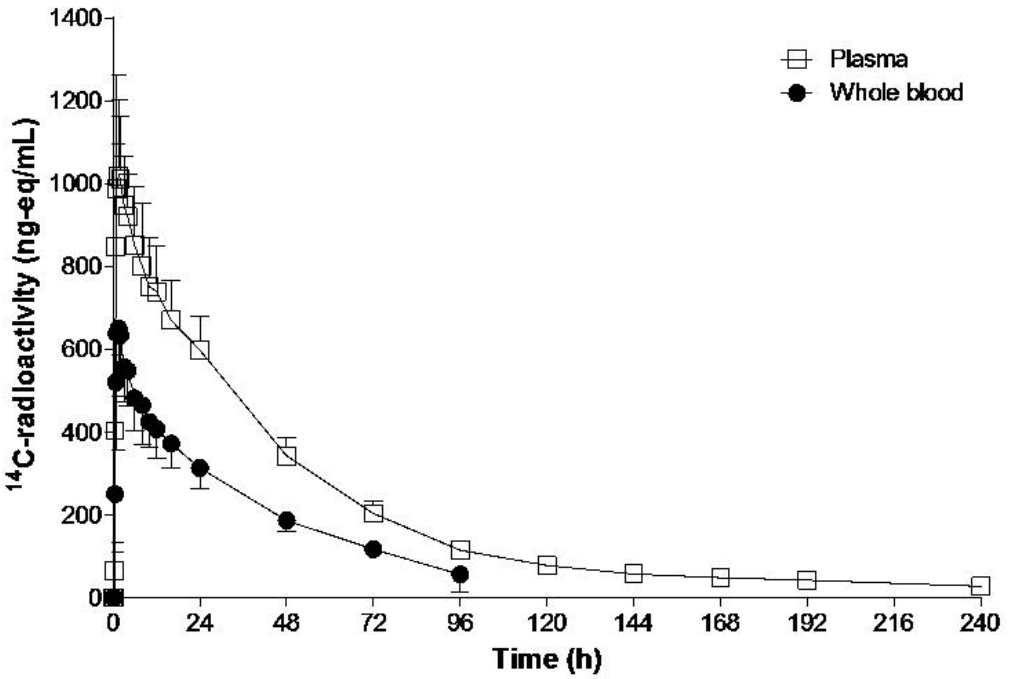
1400
1200
1000
800
600
400
200
0
$^{14}$C-radioactivity (ng-eq/mL)
0
24
48
72
96
120
144
168
192
216
240
Time (h)
Plasma
Whole blood

B

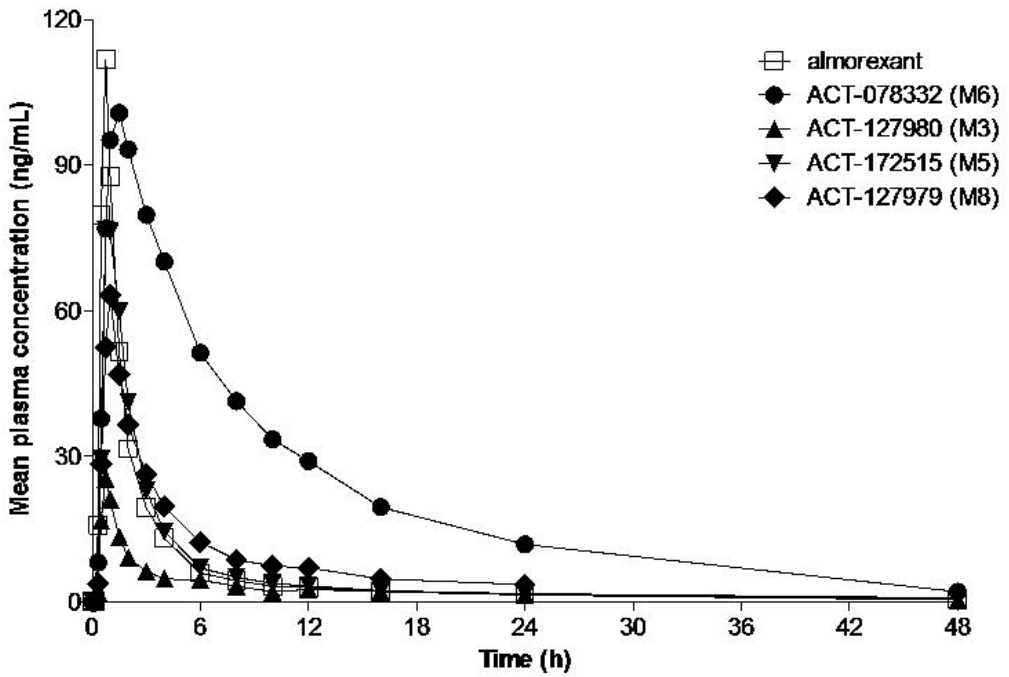
120
90
60
30
0
Mean plasma concentration (ng/mL)
0
6
12
18
24
30
36
42
48
Time (h)
almorexant
ACT-078332 (M6)
ACT-127980 (M3)
ACT-172515 (M5)
ACT-127979 (M8)

Figure 2

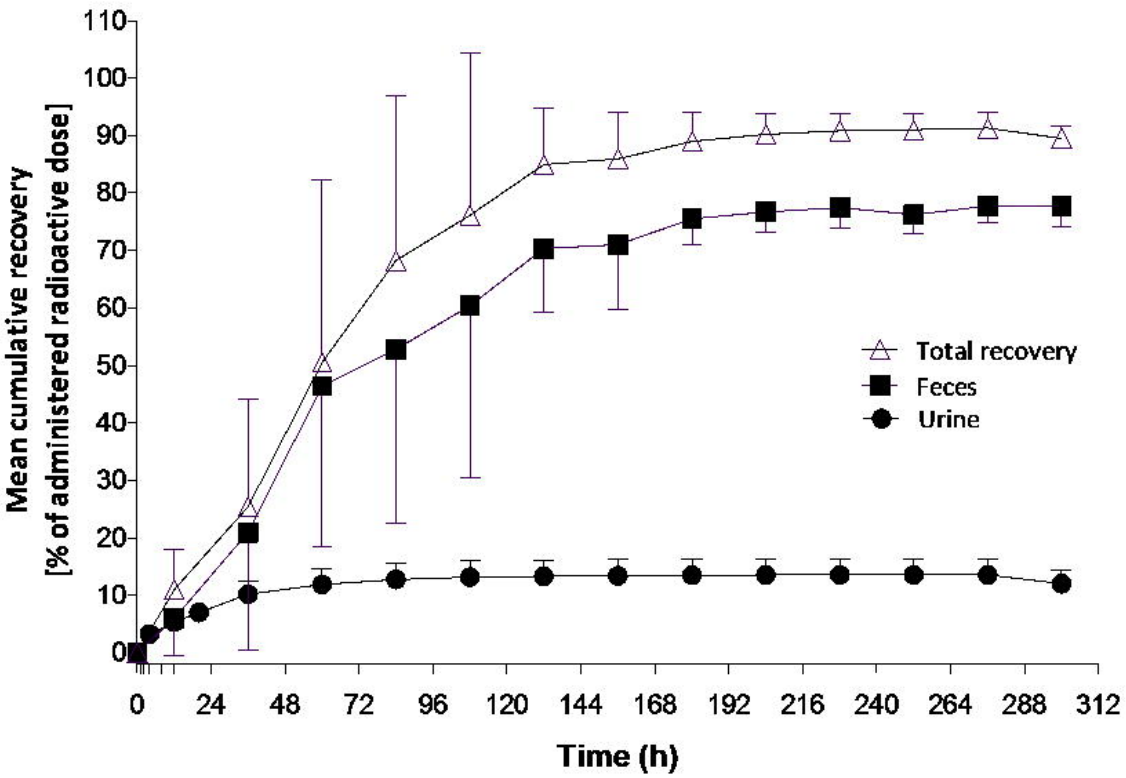
Mean cumulative recovery
[% of administered radioactive dose]
110
100
90
80
70
60
50
40
30
20
10
0
0
24
48
72
96
120
144
168
192
216
240
264
288
312
Time (h)
Total recovery
Feces
Urine

Figure 3

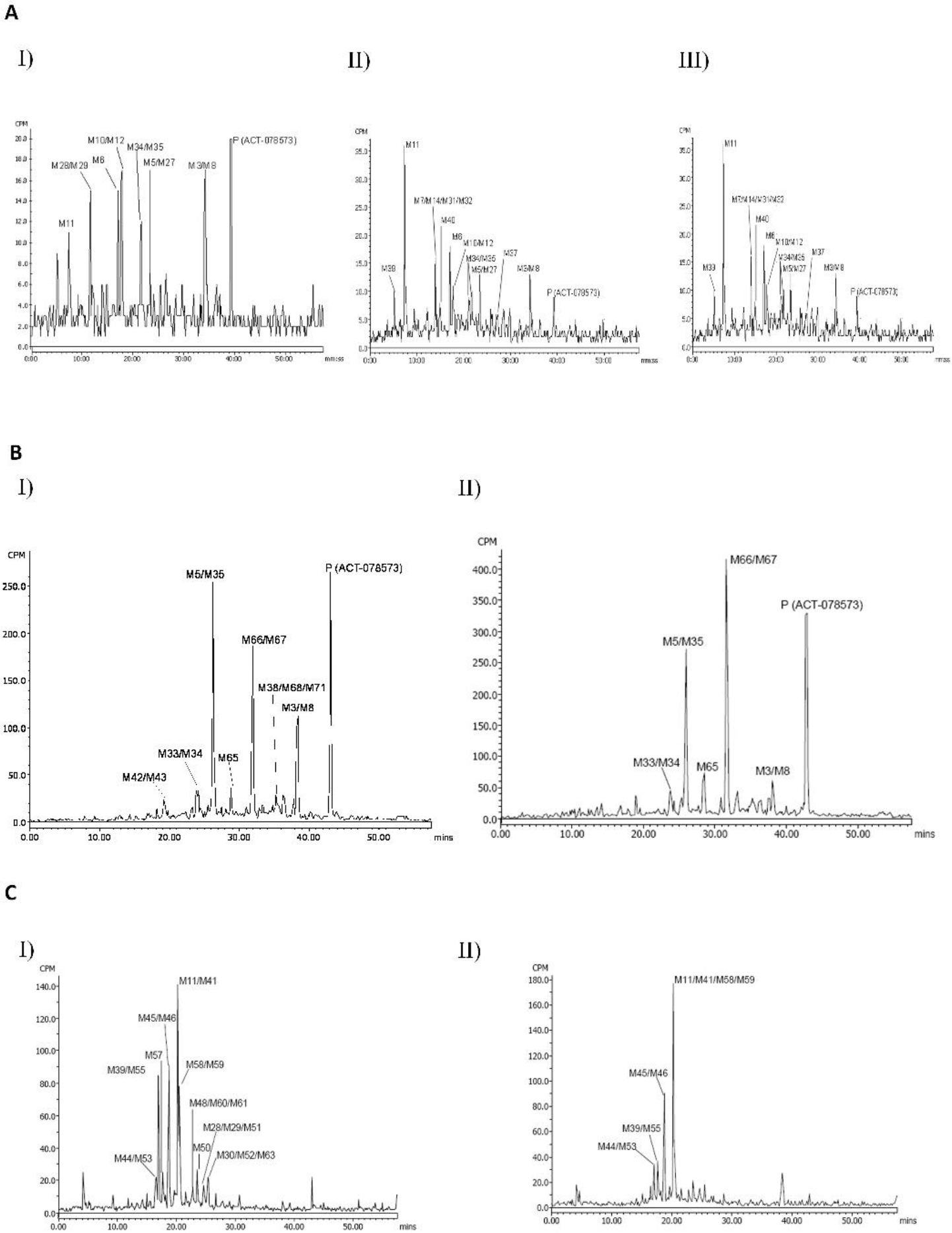
A
I)
II)
III)
CPM
M11
M28/M29
M6
M10/M12
M34/M35
M5/M27
M3/M8
P (ACT-078573)
M39
M7/M14/M31/M32
M40
M37
mm:ss
B
I)
II)
M5/M35
M66/M67
M38/M68/M71
M33/M34
M65
M42/M43
mins
C
I)
II)
M11/M41
M45/M46
M57
M39/M55
M58/M59
M48/M60/M61
M28/M29/M51
M50
M30/M52/M63
M44/M53
M11/M41/M58/M59

Figure 4

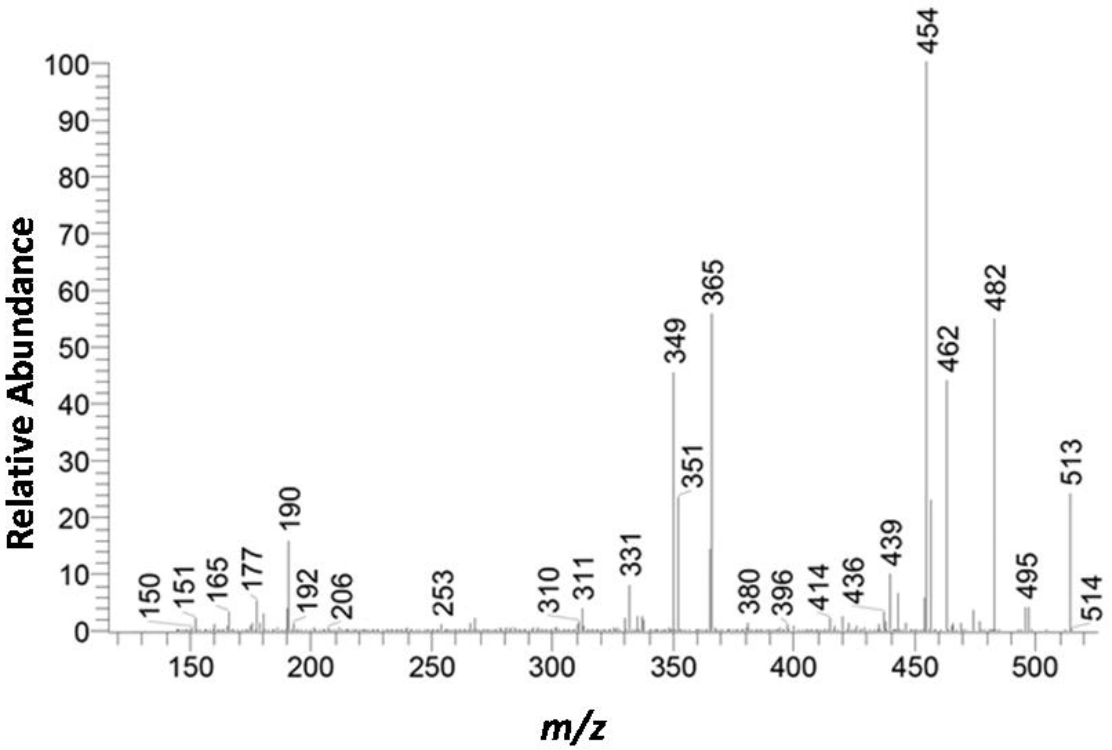
Relative Abundance
m/z
100
90
80
70
60
50
40
30
20
10
0
150
200
250
300
350
400
450
500
454
365
349
482
462
351
513
190
331
439
495
177
165
151
150
192
206
253
310
311
380
396
414
436
514

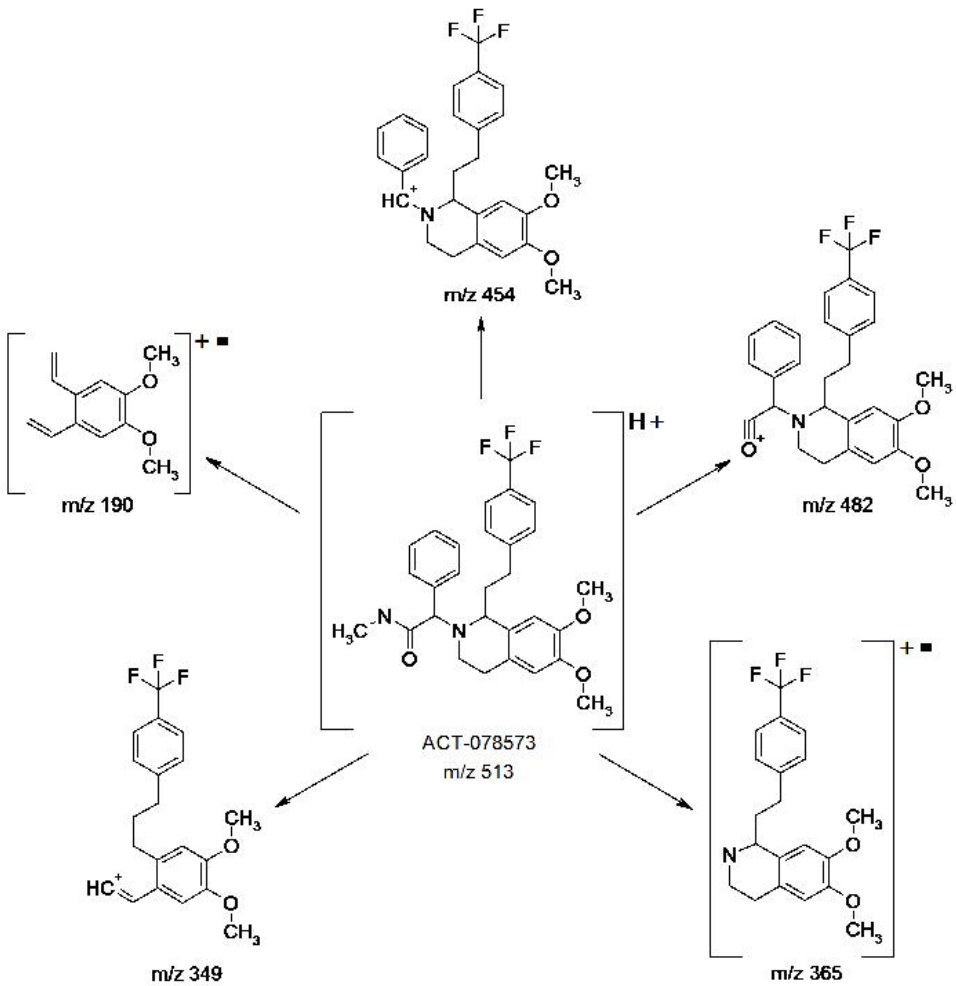
m/z 454
m/z 190
m/z 482
ACT-078573
m/z 513
m/z 349
m/z 365
H+

Figure 5

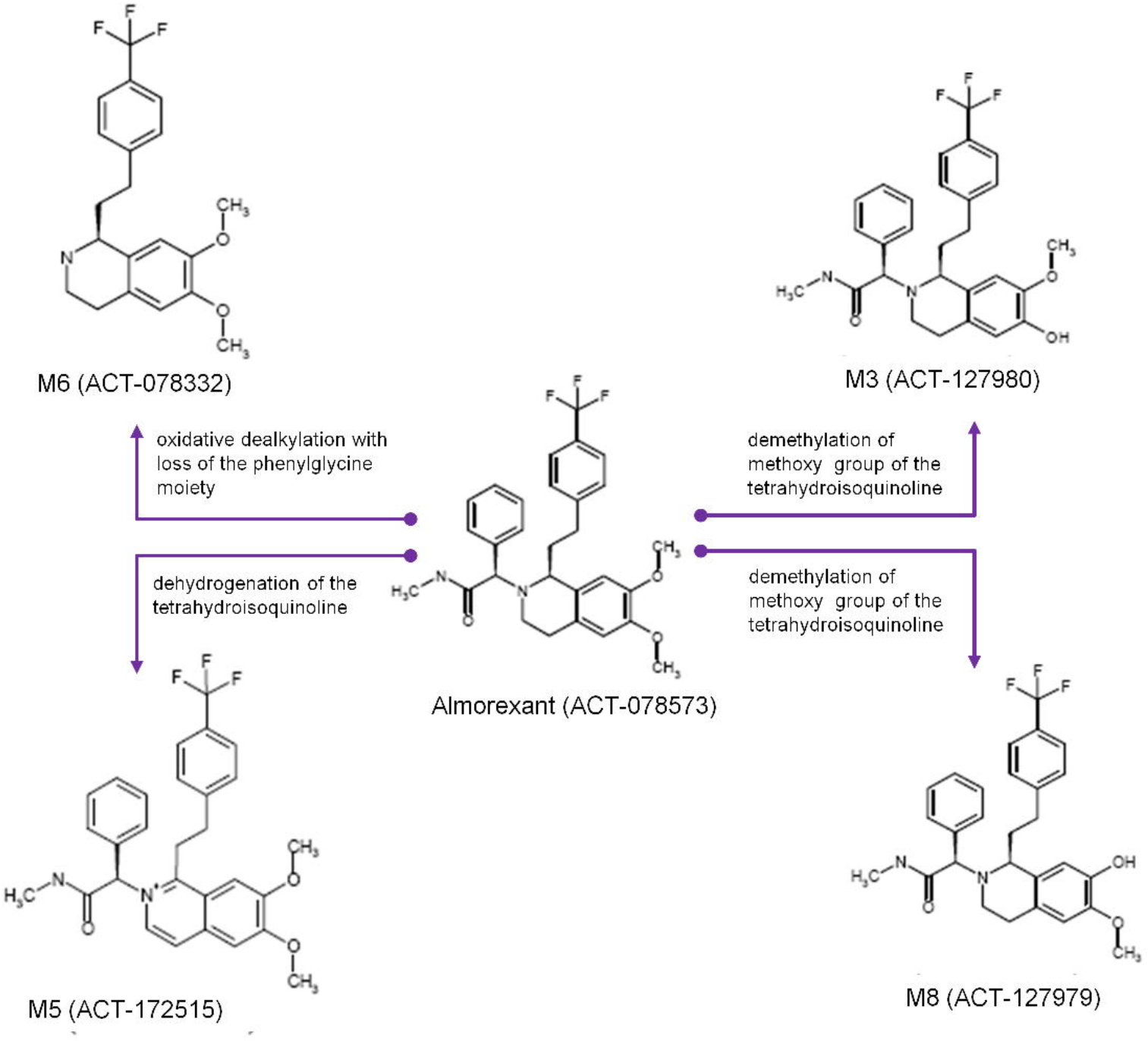
M6 (ACT-078332)
M3 (ACT-127980)
oxidative dealkylation with loss of the phenylglycine moiety
demethylation of methoxy group of the tetrahydroisoquinoline
dehydrogenation of the tetrahydroisoquinoline
demethylation of methoxy group of the tetrahydroisoquinoline
Almorexant (ACT-078573)
M5 (ACT-172515)
M8 (ACT-127979)

Figure 6

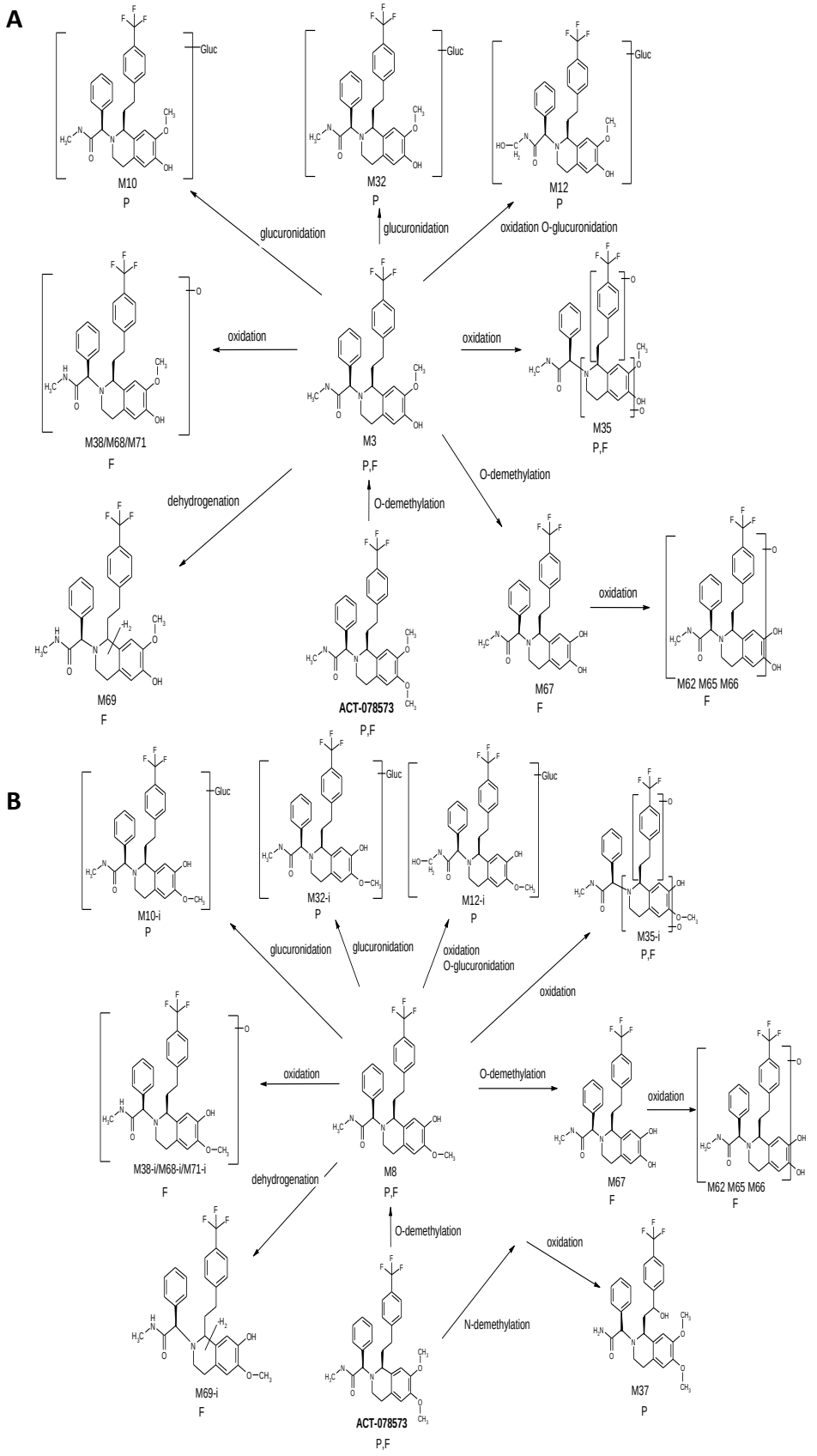
A
M10
P
M32
P
M12
P
Gluc
glucuronidation
glucuronidation
oxidation O-glucuronidation
oxidation
oxidation
M38/M68/M71
F
M3
P,F
M35
P,F
dehydrogenation
O-demethylation
O-demethylation
M69
F
ACT-078573
P,F
M67
F
oxidation
M62 M65 M66
F
B
M10-i
P
M32-i
P
M12-i
P
M35-i
P,F
glucuronidation
glucuronidation
oxidation
O-glucuronidation
oxidation
oxidation
M38-i/M68-i/M71-i
F
M8
P,F
O-demethylation
oxidation
M67
F
M62 M65 M66
F
dehydrogenation
O-demethylation
oxidation
M69-i
F
ACT-078573
P,F
N-demethylation
M37
P

Figure 6

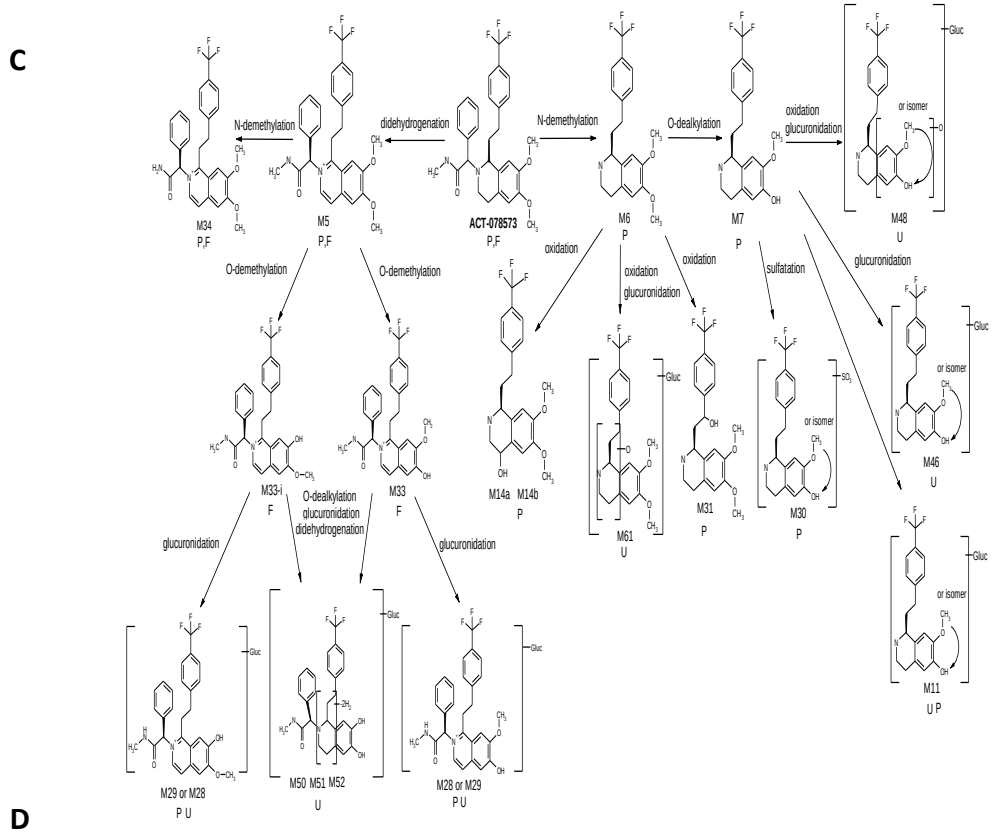
C
N-demethylation
didehydrogenation
N-demethylation
O-dealkylation
oxidation
glucuronidation
or isomer
M34
P,F
M5
P,F
ACT-078573
P,F
M6
P
M7
P
M48
U
O-demethylation
O-demethylation
oxidation
oxidation
glucuronidation
oxidation
sulfatation
glucuronidation
M33-i
F
M33
F
M14a
M14b
P
M61
U
M31
P
M30
P
M46
U
O-dealkylation
glucuronidation
didehydrogenation
glucuronidation
glucuronidation
M11
U P
M29 or M28
P U
M50 M51 M52
U
M28 or M29
P U
D
N-dealkylation
dehydrogenation
glucuronidation
ACT-078573
P,F
M6
P
M27
P
M60
U
dehydrogenation
dehydrogenation
O-dealkylation
O-dealkylation
M63
U
M63-i
U
M42
F
M43
F
glucuronidation
glucuronidation
glucuronidation
oxydation
glucuronidation
M44 or M45
U
M45 or M44
U
M41 or M39
P,U
M53/M55/M57/M58/M59
U
M39 or M41
P,U

Figure 7

A

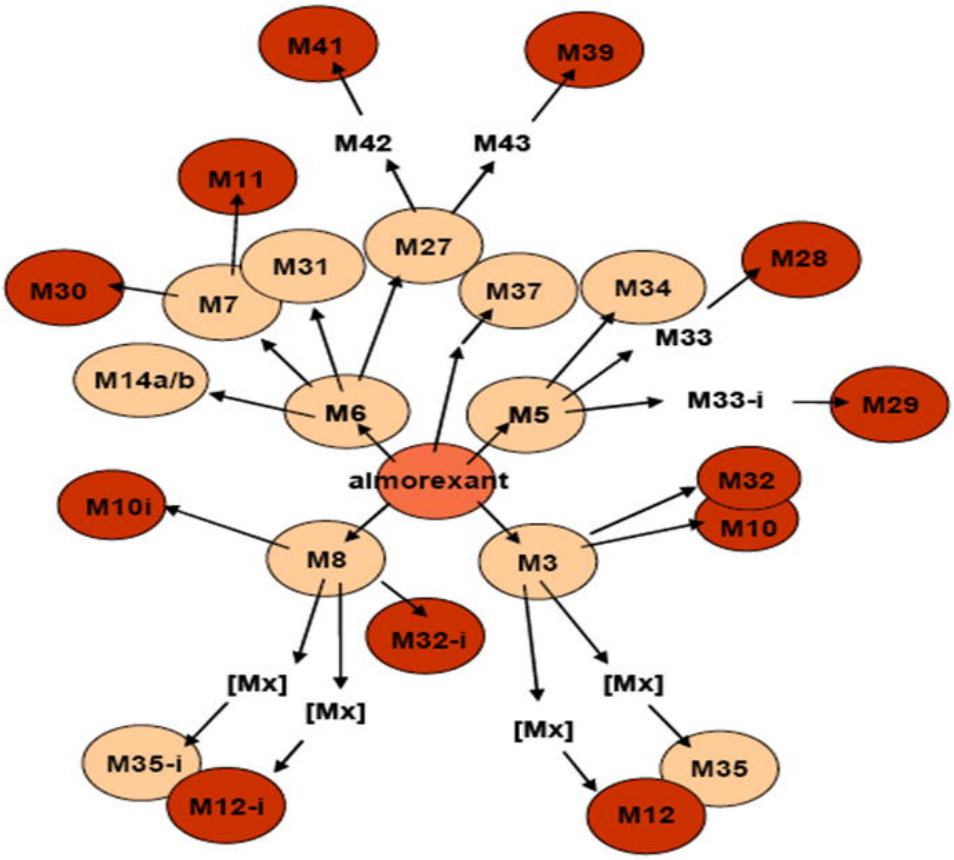
M41
M39
M42
M43
M11
M27
M31
M30
M7
M37
M34
M28
M33
M14a/b
M6
M5
M33-i
M29
almorexant
M10i
M32
M10
M8
M3
M32-i
[Mx]
[Mx]
[Mx]
[Mx]
M35-i
M12-i
M35
M12

B

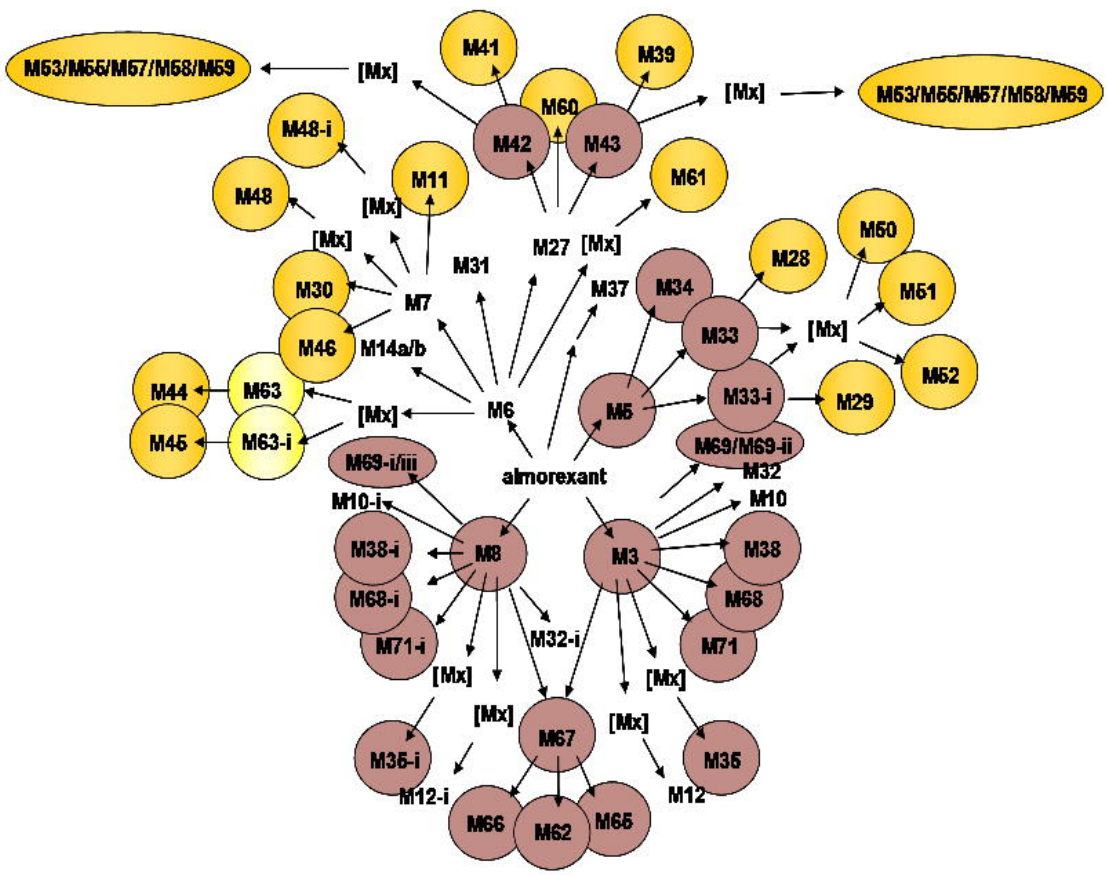
M53/M55/M57/M58/M59
[Mx]
M41
M39
[Mx]
M53/M55/M57/M58/M59
M60
M42
M43
M48-i
M11
M61
M48
[Mx]
[Mx]
M27
[Mx]
M31
M30
M7
M37
M34
M28
M60
M61
M33
[Mx]
M46
M14a/b
M52
M44
M63
M6
M5
M33-i
M29
M45
M63-i
[Mx]
M69/M69-ii
M69-i/iii
almorexant
M32
M10-i
M10
M38-i
M8
M3
M38
M68-i
M68
M71-i
M71
M32-i
[Mx]
[Mx]
[Mx]
[Mx]
M67
M35-i
M35
M12-i
M12
M66
M62
M65